Lasers in Surgery and Medicine 19:273–283 (1996)

Occurrence and Magnitude of Pressure Waves During Er:YAG Laser Ablation of Atherosclerotic Tissue: Comparison to XeCl Excimer Laser Ablation

Carsten H. Rose, Dipl-Phys, Karl K. Haase, MD, Manfred Wehrmann, MD, and Karl R. Karsch, MD

Medical Clinic, Department of Cardiology (C.H.R., K.K.H., K.R.K.) and Institute of Pathology (M.W.), Tübingen University, 72076 Tübingen, Germany

Background and Objective: **Since excimer laser ablation has not shown advantages in comparison to conventional balloon angioplasty, the search for other laser light sources came up with the Er:YAG laser, operating at a wavelength of 2.94 μm.**
Study Design/Materials and Methods: **Normal and atherosclerotic human vessel segments were irradiated in vitro, using pulsed Er:YAG laser systems. The laser beam was either focused onto the tissue in air or delivered via a fibre system onto the tissue being immersed in saline. Needle-type hydrophones were used for pressure pulse detection.**
Results: **Er:YAG laser irradiation results in effective tissue ablation of normal and calcified atherosclerotic vessel segments. In comparison to excimer lasers, ablation rates can be increased by a factor of 5 to 10 at least. Er:YAG laser ablation is also associated with a generation of pressure waves. On calcified plaque, the acoustic signals differ significantly from those on normal tissue. Histological tissue analysis reveals small zones of discoloration and tissue fissures that are found 100–200 μm lateral to the crater edge, depending on the energy density used.**
Conclusion: **Er:YAG lasers generate pressure waves that are comparable to excimer laser ablation. Er:YAG lasers, however, show a markedly improved ablation efficiency, which may favour these systems as effectively cutting, less traumatic tools for removal of atherosclerotic plaque.** © 1996 Wiley-Liss, Inc.

Key words: atherosclerosis, Er:YAG, pressure waves

INTRODUCTION

In addition to conventional methods of surgical and interventional treatment of arterial obstructive disease such as bypass operation and balloon dilatation, the use of laser angioplasty, and especially XeCl excimer laser angioplasty, has gained more interest in the last decade. In most cases, however, ablation is not selective, and normal arterial wall also will be damaged [1–3]. To avoid complications such as severe dissections or perforation of the arterial wall, an in situ discrimination between normal and atheromatous structures and a laser light source with high ablation efficiency but low vessel wall injury are desirable. In previous publications, experimental arrangements are described that employ the detection of acoustic signals during laser ablation in vitro, partly in combination with spectroscopic techniques [4–10], or other laser systems (e.g., Ho:YAG) are used for ablation [11,12]. However, further experiments regarding the acoustic and spectroscopic discrimination of vessel wall structures, as well as the introduction of new laser and

Accepted for publication August 22, 1995.

Address reprint requests to Carsten H. Rose, Institut für Halbleitertechnik, Universität Stuttgart, Breitscheidstraße 2/IV, D-70174 Stuttgart, Germany.

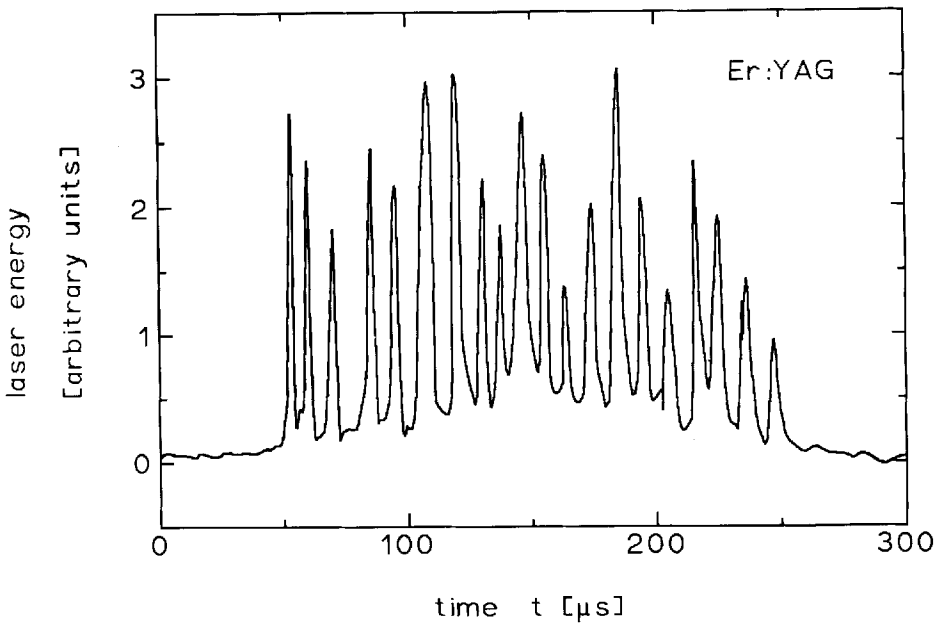

Fig. 1. Oscilloscope tracing of the energy output from an Er:YAG laser (Spectron Laser Physics, UK). The macropulse duration is ~200 μs and 20 spikes can be counted.

catheter devices, will be neccessary to surpass the standards of conventional techniques for laser angioplasty. Er:YAG laser light, which is emitted at 2.94 μm, is extremely well absorbed in water. This absorption peak results in explosive vaporization of the target material during irradiation and differs from excimer lasers that take action by absorption in proteins and molecules [13,14]. In previous studies, it was documented that excimer laser ablation is associated with a generation of pressure waves that are found in a range of 1–5 MPa (10–50 atmospheres). It was postulated that pressure wave formation in combination with low ablation rates constitute major factors for side effects that contribute to the poor clinical outcome of stand-alone excimer laser angioplasty as compared to PTCA alone. On the supposition that Er:YAG lasers might ablate atherosclerotic plaque more effectively and less traumatically than XeCl excimer lasers, this study was initiated. It, therefore, focuses on the evaluation of Er:YAG laser irradiation of calcified plaque and normal arterial wall in combination with the detection of stress waves generated during ablation. The experimental results presented here are part of a follow-up study of similar experiments performed for XeCl excimer laser ablation [4,5,15].

MATERIALS AND METHODS

For this experimental study, two Er:YAG lasers were used as laser light sources (Spectron Laser Physics, UK, for transmission in air and MCL 29, Aesculap Meditec, Germany, for fibre transmission). Both lasers operate at a wavelength of 2.94 μm in a free-running spiking mode and produce macropulses of ~200 μs duration with 15–20 spikes per pulse (Fig. 1) and an energy of up to 150 mJ per pulse. The laser beam was either focused by a lens onto the tissue (Spectron Laser Physics) or into a 600-μm core diameter zirconiumfluoride fibre (Le Verre Fluore, F) with a quartz tip of 360-μm core diameter and then delivered onto the tissue (MCL 29, Aesculap Meditec) with the fibre in contact with the tissue. In both cases, the laser spot diameter was adjusted to a size of 350 μm ± 50 μm; the lasers were operated in a single-shot mode. The pulse energy was measured by means of a photodiode joule meter (EM 1 with ED 500, Gentec, CDN) and was kept constant at 150 J/cm^2 ± 15 J/cm^2 throughout the whole series.

The acoustic experiments were conducted using specimens from 14 human aortas retrieved 24 hours postmortem. If necessary, they were frozen and stored at low temperature (−4°C) until use. Samples of ~20 × 20 mm^2 size with either calcified hard plaques or normal areas of arterial wall were identified by macroscopic inspection before testing for signals. This identification was checked and verified by micropathological means after the experiments. The pathological examination also confirmed the assumption that the en-

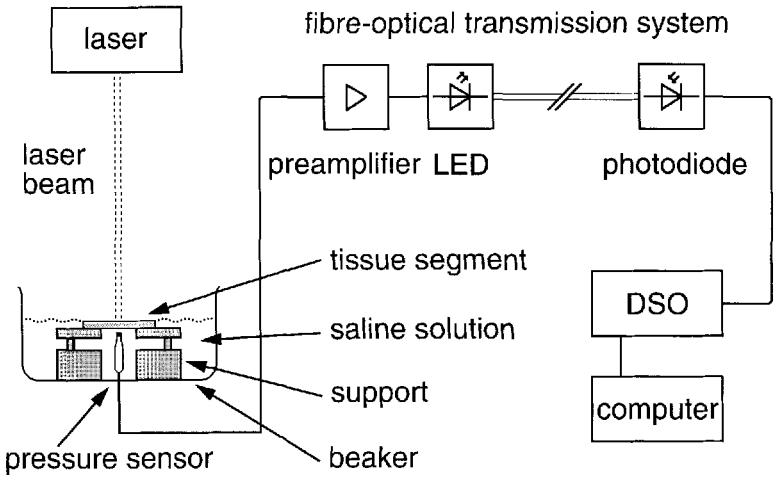

Fig. 2. Experimental arrangement for monitoring and analyzing acoustic signals during Er:YAG laser ablation in air.

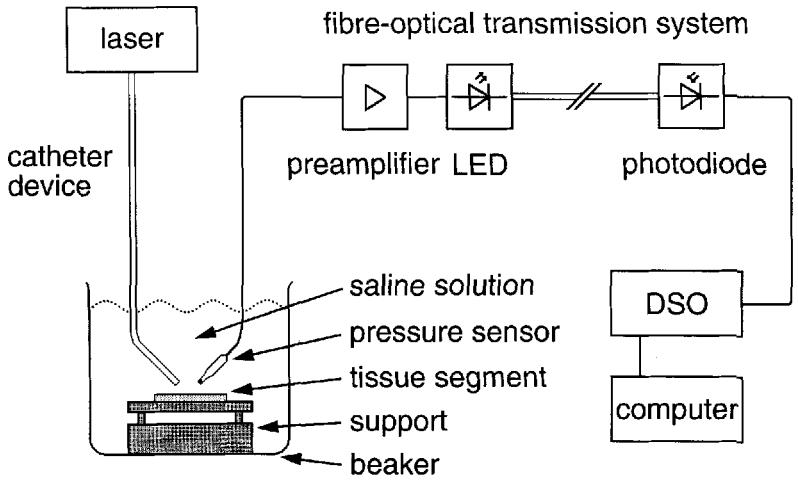

Fig. 3. Experimental arrangement for monitoring and analyzing acoustic signals during Er:YAG laser ablation in normal saline solution.

ergy density used was sufficient, i.e., each specimen showed significant ablation craters after the application of laser energy. The tissue samples were mounted onto a 50 × 60 mm^2, 3-mm-thick lucite plate fastened to a metal support by spacers of 30 mm length. The specimens were placed in a beaker filled with a normal saline solution (0.9% w/v NaCl), either with the tissue at the surface of the saline solution and the laser beam focused onto it (Fig. 2), or in the saline solution and the laser fibre directed into the beaker in contact with the tissue sample (Fig. 3). In the first case, the hydrophone was placed beneath the tissue with contact to it (Fig. 2), in the second case, the distance between the hydrophone and the tissue sample was set to the same order of magnitude as that of the fiber tip in order to avoid any perturbation of the acoustic signal. During the measurements, no dependence of the acoustic signal on the position of the fiber could be observed, as long as the fiber tip did not affect the free propagation of the pressure pulse (Fig. 3).

The acoustic signals generated by the laser pulses were measured with needle-type hydrophones (Institute of Semiconductor Engineering, Stuttgart University, Stuttgart, Germany). These transducers are manufactured from a 0.5 mm diameter, 9-μm-thick polyvinylidenefluoride (PVDF) piezoelectric film mounted onto a 0.5-mm-thick metal needle. The hydrophones have a responsivity between 30 and 50 μPa/V and a frequency response up to 20 MHz. The shortest rise

time measured for these types of hydrophones was 30 ns. The hydrophone was typically placed 0.5 mm to 2.0 mm from the center of ablation; this distance was adjusted in order to obtain a sufficient signal and to avoid saturation when using a broadband fiber-optic transmission system (Institute of Semiconductor Engineering). To account for the different hydrophone locations, the experimental results presented here are normalized to a standard distance of 1 mm, assuming an acoustic signal that is inversely proportional to the distance. During the measurements, the acoustic signals did not show any significant directionality and the directivity pattern of the hydrophone was accounted for by placing its disk like sensing area perpendicular to the propagation direction of the sound wave.

The acoustic signals were recorded on a dual channel digital storage oscilloscope (PM 3323, Philips, NL); the data were transferred to a personal computer for processing and storing. The pressure pulses were analyzed in the time domain with regard to peak pressure, rise time, and pressure increase. The peak pressure is defined as the pressure interval between 0% and 100% of the maximum pressure, and the rise time is defined as the time interval between 10% and 90% of the maximum pressure. The pressure increase is calculated by dividing the peak pressure by the rise time.

Pressure wave analysis was performed only at energy densities above the ablation threshold. Acoustic signals generated below ablation threshold were not registered in this study, because there is no direct impact for the analysis of such stress waves without ablation taking place.

Statistical evaluation was performed by analyzing the differences in peak pressure, rise time, and pressure increase for ablation of normal arterial wall and calcified plaque in air and in saline solution using the Student's t-test. P values <0.05 were considered to be statistically significant.

In order to achieve ablation rates for normal as well as atherosclerotic tissue samples, perforation experiments were conducted in air. Ablation was continued with the number of pulses counted until the tissue sample was perforated. Perforation was detected when a photodiode joule meter (EM 1 with ED 500, Gentec, CDN) placed behind the tissue sample gave a signal of at least 50% of the intensity of the emitted laser energy. The thickness of the tissue samples was measured with an ultrasonic transducer system (Cornea Gage II, Sonogage, USA). Measurements of the ablation rates in saline solution were not conducted because Er:YAG laser light is strongly absorbed by water, which complicates simultaneous measurements of ablation rates and pressure waves. All fibre measurements presented in this study were performed in a contact mode without using a force, so as to avoid mechanical side effects.

After the experiments, the tissue samples were immersed in 10% neutral-buffered formalin, dehydrated, and embedded in paraffin. Histological sections were assessed from the arterial segments close to the laser treated area using standard hematoxylin and eosin and elastica van Gieson stains. Tissue damage was defined as carbonization, discoloration, vacuoles, fissures, and fractures. The extent of tissue damage is given in micrometers, including standard deviation.

RESULTS

Figures 4 and 5 show two typical pressure pulses recorded during the experiments in air and saline, respectively. The pulses with the higher peak pressure represent the acoustic signals obtained on hard atheromatous plaque, and the other ones those obtained on smooth normal arterial wall. The difference between both signals is obvious: the pulses on calcified plaque exhibit higher peak pressures ($p_{peak} \approx 0.29$ MPa in air; $p_{peak} \approx 0.75$ MPa in saline) and shorter rise times ($t_{rise} \approx 300$ ns in air; $t_{rise} \approx 130$ ns in saline). The pulses on normal tissue show lower peak pressures ($p_{peak} \approx 0.15$ MPa in air; $p_{peak} \approx 0.55$ MPa in saline) and longer rise times ($t_{rise} \approx 900$ ns in air; $t_{rise} \approx 420$ ns in saline). The discrimination between these two types of acoustic signals is facilitated by examining the rate of pressure increase (on calcified plaque: $rate_{p.i.} \approx 0.97$ kPa/ns in air and $rate_{p.i.} \approx 5.77$ kPa/ns in saline; on normal tissue: $rate_{p.i.} \approx 0.17$ kPa/ns in air and $rate_{p.i.} \approx 1.31$ kPa/ns in saline). Thus by analyzing pressure increase and rise time of the acoustic signals, the pulse shape, whether bipolar or unipolar, becomes less important for the discrimination of plaque and normal vessel wall.

Figures 6 and 7 show the analysis of multiple single laser pulse shots on calcified and on normal arterial wall recorded in air and normal saline solution, respectively. The test data received from hard plaque are marked by a square and those from normal arteries by a rhomb. Figure 6 presents the data from Er:YAG laser ablation in air. On calcified plaque ($n = 11$; index

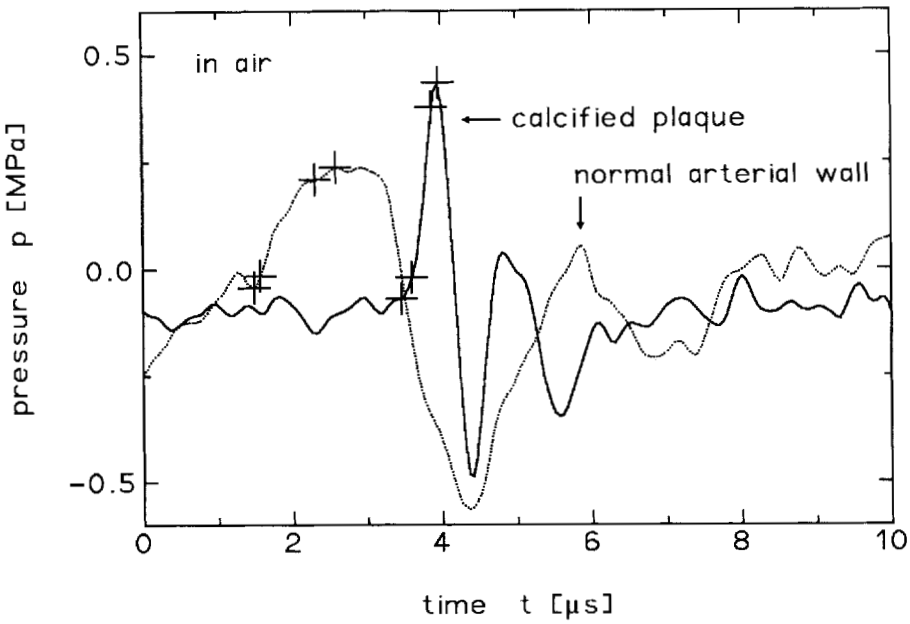

Fig. 4. Acoustic signals of hard calcified plaque (solid line, $t_{rise} \approx 300$ ns, $p_{peak} \approx 0.29$ MPa) and of soft normal arterial wall (dotted line, $t_{rise} \approx 900$ ns, $p_{peak} \approx 0.15$ MPa) during Er:YAG laser ablation in air (laser energy 150 J/cm^2, spot diameter 350 μm). In both graphs the pressure levels corresponding to 0%, 10%, 90%, and 100% are marked by a cross (cf. Materials and Methods).

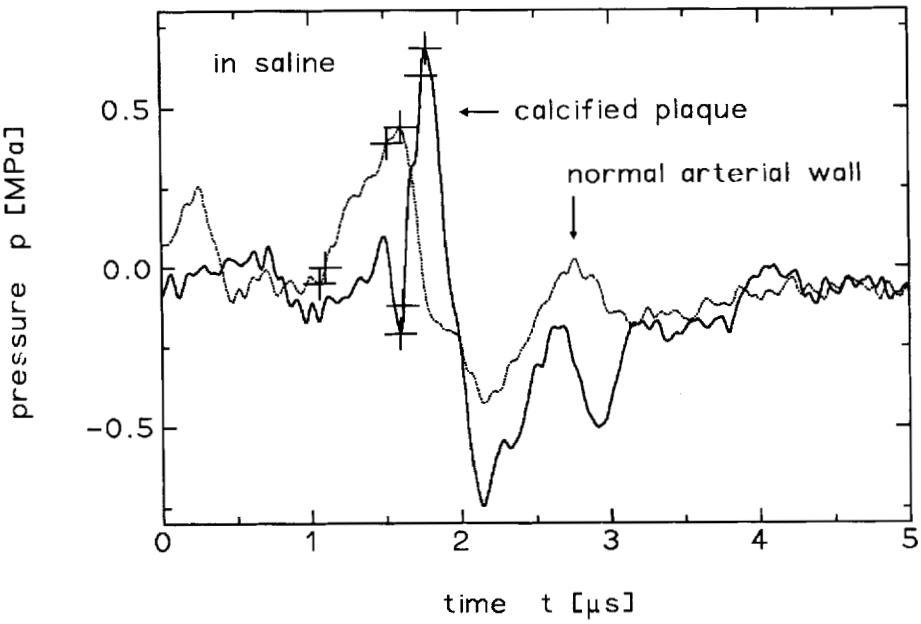

Fig. 5. Acoustic signals of hard calcified plaque (solid line, $t_{rise} \approx 130$ ns, $p_{peak} \approx 0.75$ MPa) and of soft normal arterial wall (dotted line, $t_{rise} \approx 420$ ns, $p_{peak} \approx 0.55$ MPa) during Er:YAG laser ablation in saline solution (laser energy 150 J/cm^2, spot diameter 350 μm). In both graphs the pressure levels corresponding to 0%, 10%, 90%, and 100% are marked by a cross (cf. Materials and Methods).

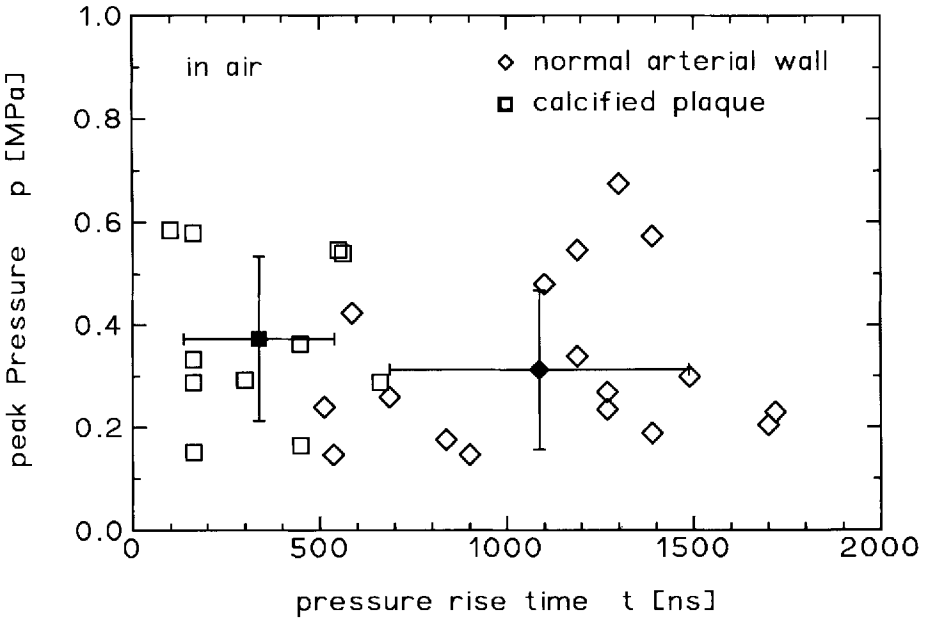

Fig. 6. Analysis of acoustic signals received after single pulse Er:YAG laser irradiation of human vascular tissue in air (laser energy 150 J/cm^2, spot diameter 350 μm). Specimens with calcified plaque (t_{rise} = 340 ns ± 200 ns, p_{peak} = 0.37 MPa ± 0.16 MPa) show a significantly shorter rise time ($P < 0.001$) than those with normal arterial wall (t_{rise} = 1090 ns ± 400 ns, p_{peak} = 0.31 MPa ± 0.16 MPa), while peak pressures are compareable ($P > 0.1$). The filled symbols with standard deviations represent mean values in accordance to Table 1.

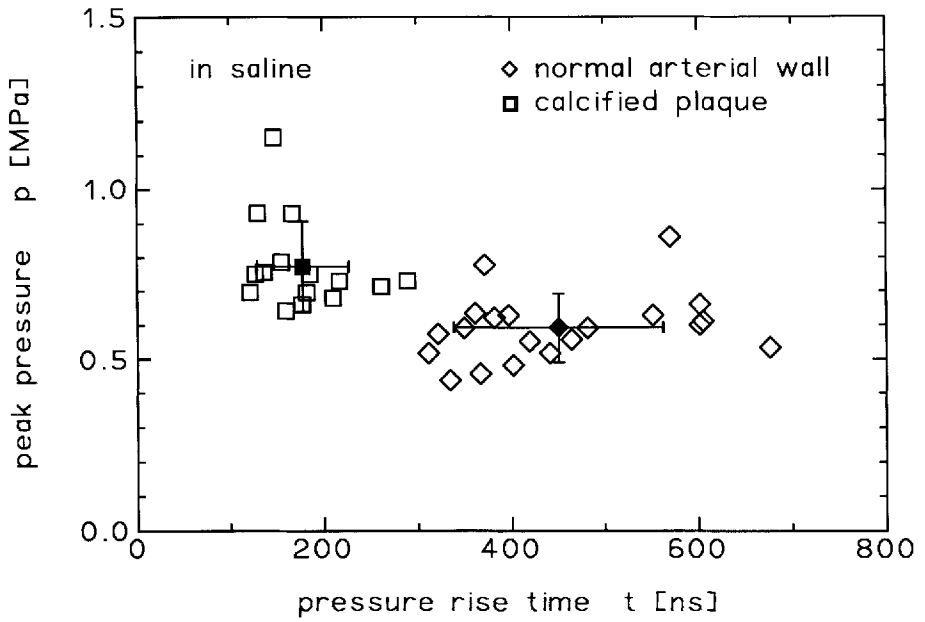

Fig. 7. Analysis of acoustic signals received after single pulse Er:YAG laser irradiation of human vascular tissue in saline solution (laser energy 150 J/cm^2, spot diameter 350 μm). Specimens with calcified plaque (t_{rise} = 180 ns ± 50 ns, p_{peak} = 0.78 MPa ± 0.13 MPa) show both a significantly shorter rise time ($P < 0.001$) and a significantly higher peak pressure ($P < 0.001$) than those with normal arterial wall (t_{rise} = 450 ns ± 110 ns, p_{peak} = 0.59 MPa ± 0.10 MPa). The filled symbols with standard deviations represent mean values in accordance to Table 1.

Table 1. Peak Pressure, Pressure Rise Time, Pressure Increase Rate for Normal Arterial Wall and Calcified Plaque When Ablating with Er:YAG Laser in Air and Saline Solution, Respectively*

Er:YAG	in air		in saline	
	normal arterial wall	calcified plaque	normal arterial wall	calcified plaque
number of measurements	18	11	20	15
maximum pressure [MPa]	0.31 ± 0.16	0.37 ± 0.16	0.59 ± 0.10	0.78 ± 0.13
rise time [ns]	1090 ± 400	340 ± 200	450 ± 110	180 ± 50
pressure increase [kPa/ns]	0.3 ± 0.2	1.7 ± 1.6	1.4 ± 0.3	4.7 ± 1.6

*Laser energy 150 J/cm^2, spot diameter 350 μm.

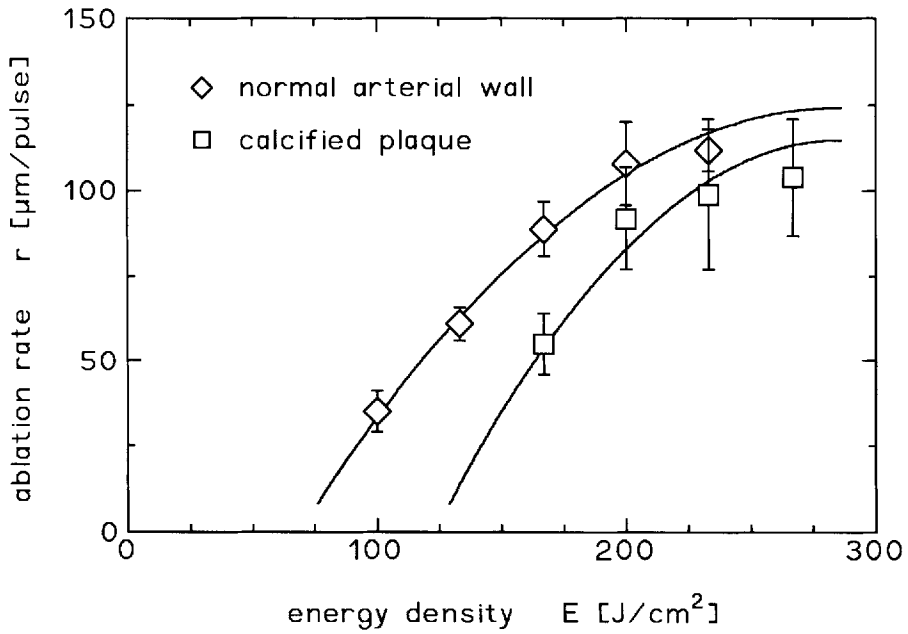

Fig. 8. Ablation rate versus energy density for normal arterial wall and calcified plaque when ablating in air. Note that the ablation rates for normal tissue are higher than those for calcified tissue. If plaque and normal tissue are being irradiated at the same time, normal arterial wall will be preferentially ablated.

c.p.), the acoustic signals differ significantly from those on normal tissue (n = 18; index n.t.) with regard to pressure rise times ($t_{rise,c.p.}$ = 340 ns ± 200 ns vs. $t_{rise,n.t.}$ = 1090 ns ± 400 ns; $P < 0.001$), whereas peak pressures ($p_{peak,c.p.}$ = 0.37 MPa ± 0.16 MPa vs. $p_{peak,n.t.}$ = 0.31 MPa ± 0.16 MPa; $P > 0.1$) are comparable. Figure 7 presents the data from Er:YAG laser ablation in physiological saline solution. On calcified plaque (n = 15; index c.p.), the acoustic signals differ significantly from those on normal tissue (n = 20; index n.t.) with regard to pressure rise times ($t_{rise,c.p.}$ = 180 ns ± 50 ns vs. $t_{rise,n.t.}$ = 450 ns ± 110 ns; $P < 0.001$), and peak pressures ($p_{peak,c.p.}$ = 0.78 MPa ± 0.13

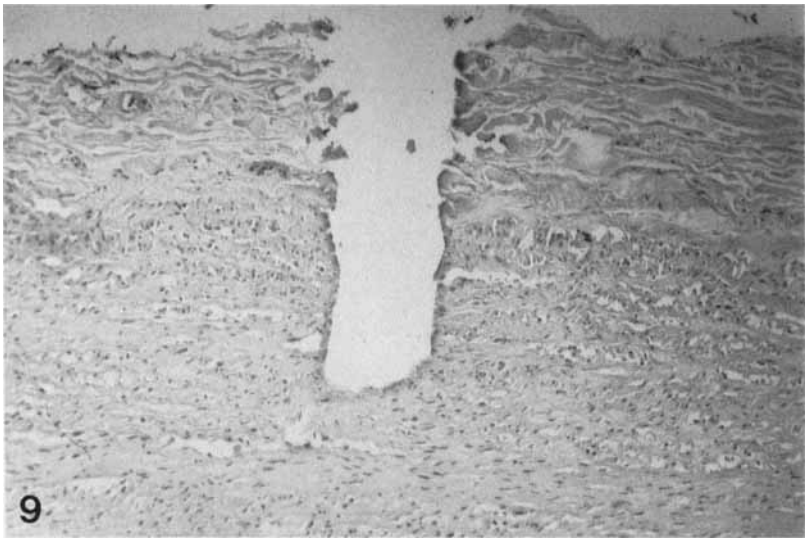

Fig. 9. Photomicrograph of fibrous aortic wall irradiated in saline solution showing a crater produced with an energy fluence of 100 J/cm^2. The laser spot diameter was 350 μm; five laser pulses were given. Laser ablation produced a sharp crater edge with only minimal changes in the adjacent tissue (hematoxylin-eosin stain, ×20).

MPa vs. $p_{peak,n.t.}$ = 0.59 MPa ± 0.10 MPa; $P <$ 0.001).

The scattering of the experimental results is attributed to the natural heterogeneity of human aortas and to varying degrees of calcification of the investigated atheromatous vessels. The different mechanical properties of hard calcified plaque and soft normal arterial wall result in different acoustic impedances. This leads to differences in the acoustic coupling of the vessels to a medium like saline solution or blood: when ablating hard plaque, most of the acoustic signal will be reflected into the medium, whereas soft arterial wall is acoustically better matched, i.e., the acoustic signal will propagate into the tissue as well as into the medium.

The ablation rates measured for ablation in air (Fig. 8) proved that the energy density was sufficiently high. Ablation rates between <50 and >100 μm per pulse were achieved and are in good accordance with other findings [13,16]. It should be pointed out that the ablation rate of normal tissue (89 μm/pulse ± 8 μm/pulse; n = 20) is significantly higher ($p < 0.001$) than that of calcified plaque (55 μm/pulse ± 9 μm/pulse; n = 15) at a

Fig. 10. Photomicrograph of fibrous aortic wall. This crater was produced using an energy fluence of 200 J/cm^2. The laserspot diameter was 350 μm; five laser pulses were given. An intense zone of discoloration around the crater margin is seen, which is more pronounced as compared to Figure 9. Note some fissures and small cracks lateral to the crater lumen, which extend 100–200 μm into the surrounding tissue (hematoxylin-eosin stain, × 40). Vacuoles are not seen on both photomicrographs.

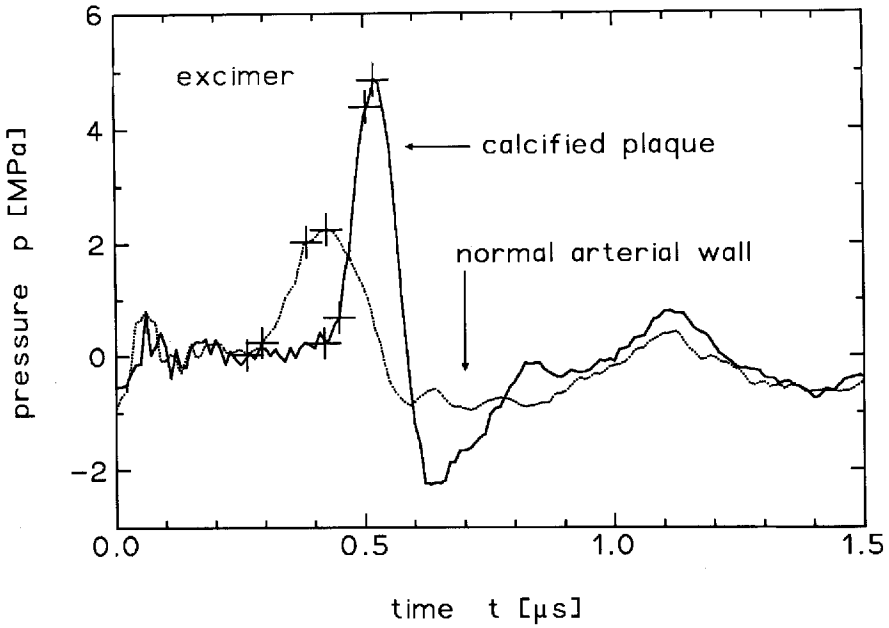

Fig. 11. Acoustic signals of hard calcified plaque (solid line, $t_{rise} \approx 58$ ns, $p_{peak} \approx 4.3$ MPa) and of soft normal arterial wall (dotted line, $t_{rise} \approx 86$ ns, $p_{peak} \sim 2.0$ MPa) during XeCl excimer laser ablation in saline solution (laser energy 60 mJ/mm^2, spot diameter 600 μm). In both graphs the pressure levels corresponding to 0%, 10%, 90%, and 100% are marked by a cross (cf. Materials and Methods).

given energy density (e.g., 170 J/cm^2). As shown in Figure 8, this is valid for energy densities between 100 and 300 J/cm^2. Thus if a laser pulse happens to be irradiating a mixture of plaque and normal arterial wall, normal arterial wall will be preferentially ablated.

Histological tissue analysis revealed only small injury of crater adjacent tissue structures. A distinct zone of crater edge discoloration was observed in all tissue samples, independent of the tissue type irradiated. Fissures and small fractures (fracture width < 50 μm) were seen in all calcified samples, but in only one normal aorta. Carbonization or vacuoles were absent. Maximal tissue damage was 210 μm ± 56 μm for calcified vessel segments and 186 μm ± 51 μm for normal vessel wall (Figs. 9, 10).

DISCUSSION

A comparison of Er:YAG laser ablation to prior experiments with excimer lasers [4,5,15] reveals major similarities with respect to the pressure waves that are generated. Figure 11 shows two typical pressure pulses recorded during XeCl excimer laser ablation of tissue immersed in physiological saline solution. The experimental setup was similar to that described in Figure 3, with the exception of the laser light source (MAX 10, Technolas, energy density 60 mJ/mm^2) and the transmitting fibre (quartz, spot diameter 600 μm). Ablation of hard calcified plaque is characterized by a higher peak pressure ($p_{peak} \approx 4.3$ MPa) and a shorter rise time ($t_{rise} \approx 58$ ns), whereas ablation of soft normal arterial wall exhibits a lower peak pressure ($p_{peak} \approx 2.0$ MPa) and a longer rise time ($t_{rise} \approx 86$ ns). Figure 12 shows the analysis of multiple single XeCl excimer laser shots on calcified and normal arterial wall in saline solution. Data received from hard plaque are marked by a square and those from normal arteries by a rhomb. On calcified plaque (n = 83; index c.p.) the acoustic signals differ significantly from those on normal tissue (n = 81; index n.t.) with regard to pressure rise times ($t_{rise,c.p.} = 70$ ns ± 26 ns vs. $t_{rise,n.t.} = 163$ ns ± 43 ns; $P < 0.001$), and peak pressures ($p_{peak,c.p.} = 2.02$ MPa ± 1.16 MPa vs. $p_{peak,n.t.} = 1.28$ MPa ± 0.85 MPa; $P < 0.01$).

From a statistical point of view, it can be stated that it is possible to discriminate between calcified plaque and noncalcified tissue by using the analysis of the pressue wave signal for both Er:YAG and XeCl excimer lasers. Thus the pref-

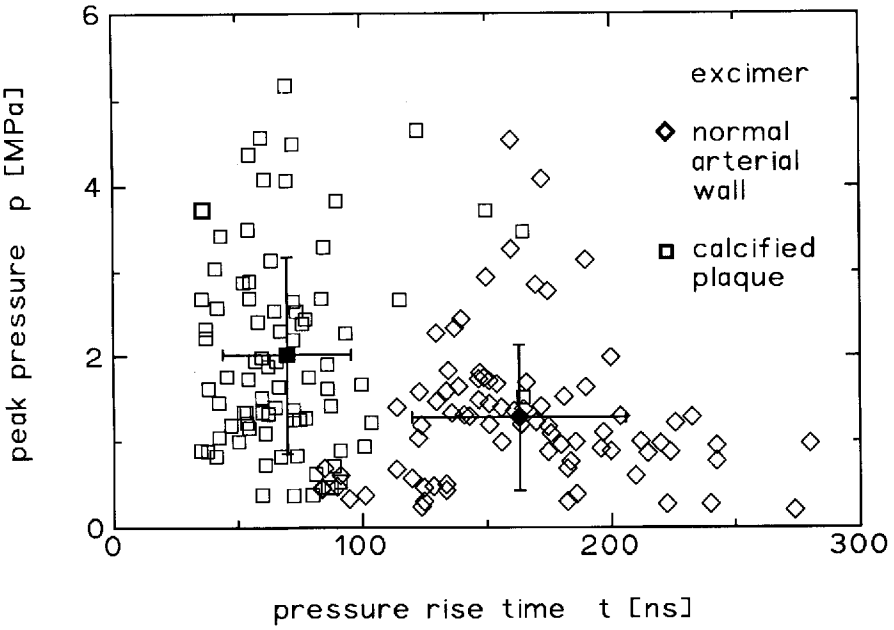

Fig. 12. Analysis of acoustic signals received after single pulse XeCl excimer laser irradiation of human vascular tissue in saline solution (laser energy 60 mJ/mm^2, spot diameter 600 μm). Specimens with calcified plaque (t_{rise} = 70 ns ± 26 ns, p_{peak} = 2.02 MPa ± 1.16 MPa) show both a significantly shorter rise time ($P < 0.001$) and a significantly higher peak pressure ($P < 0.01$) than those with normal arterial wall (t_{rise} = 163 ns ± 43 ns, p_{peak} = 1.28 MPa ± 0.85 MPa). The filled symbols with standard deviations represent mean values in accordance with Table 2.

erential ablation of normal arterial wall can be detected and the risk of uncontrolled ablation of the arterial wall and perforation of the artery might be reduced. Up to date, however, this is only valid for preselected specimens in vitro and several laser pulses delivered and may turn out to be very difficult when ablating a mixture of calcified plaque, fatty plaque and normal arterial wall in vivo.

It is, therefore, open to question if the experimental results presented above may lead to the clinical application of Er:YAG laser angioplasty with acoustic ablation control. A realtime monitoring system, consisting of an intraluminal fiber bundle with a miniature hydrophone at its tip and an oscilloscope, might facilitate the desirable discrimination between calcified plaque and noncalcified arterial wall. It is doubtful, however, if a more detailed discrimination of the variety of atherosclerotic plaque can be achieved.

It also has to be taken into consideration that flexible, nontoxic fibres for Er:YAG laser light transmission are one of the presuppositions for percutaneous transluminal applications. Such fibres are currently not available, although recent progress in fibre technology may create waveguide constructions that might be used for 2.8–3.0 μm light transmission.

Table 2. Peak Pressure, Pressure Rise Time, Pressure Increase Rate for Normal Arterial Wall and Calcified Plaque When Ablating with XeCl Excimer Laser in Saline Solution*

XeCl excimer	in saline	
	normal arterial wall	calcified plaque
number of measurements	81	83
maximum pressure [MPa]	1.28 ± 0.85	2.02 ± 1.16
rise time [ns]	163 ± 43	70 ± 26
pressure increase [kPa/ns]	8.2 ± 5.4	32.3 ± 21.3

*Laser energy 60 mJ/mm^2, spot diameter 600 μm.

Prior studies with excimer lasers have documented that pressure waves and bubble formations can cause severe dissections and perforation

of the treated vessel segments [17]. Er:YAG laser ablation is also associated with the occurance of pressure waves, which may constitute a major limitation of this technique. It has to be stated, however, that the magnitude of these pressure waves is comparably lower than those of excimer laser systems, although ablation efficiency is considerably improved for 2.94 μm irradiation. An increased cutting depth in combination with good ablation quality may contribute to a less traumatic ablation process with fewer complications at high ablation rates. Thus, Er:YAG laser irradiation may provide an alternative laser light source as an effectively cutting, less traumatic tool for removal of atherosclerotic plaque.

ACKNOWLEDGMENTS

The authors gratefully acknowledge the support during Er:YAG laser measurements by B. Jean, Department of Ophthalmology, Tübingen University, and R. Steiner, Institute for Laser Technologies in Medicine, Ulm University. This work is supported by grant of the Deutsche Forschungsgemeinschaft, Bonn.

REFERENCES

1. Choy DSJ, Stertzer SH, Myler RD, Marco J, Fournay G. Human coronary laser recanalization. Clin Cardiol 1984; 7:377–381.
2. Prince MR, Anderson RR, Deutsch TF, La Muraglia GM. Pulsed laser ablation of calcified plaque. Proc Soc Photo-Optical Instru Eng 1988; 906:305–309.
3. Isner JM, Donaldson RF, Funai JT, Deckelbaum LJ, Pandian NG, Clarke RH, Kanstan MA, Salem DN, Serenstein JS. Factors contributing to perforations resulting from laser coronary angioplasty: Observations in an intact human post mortem preparation of interoperative laser angioplasty. Circulation 1985; 72 (Suppl. II):191.
4. Crazzolara H, von Münch W, Rose CH, Thiemann U, Haase KK, Ritter M, Karsch KR. Analysis of the acoustic response of vascular tissue irradiated by an ultraviolet laser pulse. J Appl Phys 1991; 70:1847–1849.
5. Haase KK, Hanke H, Baumbach A, Hassenstein S, Wehrmann M, Duda S, Rose CH, von Münch W, Karsch KR. Occurrence, extent, and implications of pressure waves during excimer laser ablation of normal arterial wall and atherosclerotic plaque. Lasers Surg Med 1993; 13:263–270.
6. Cross FW, Al-Dhahir RK, Dyer PE. Ablative and acoustic response of pulsed UV laser-irradiated vascular tissue in a liquid environment. J Appl Phys 1988; 64:2194–2201.
7. Chen QX, Davies A, Dewhurst RJ, Payne PA. Photoacoustic probe for intra-arterial imaging and laser therapy Electr Lett 1993; 29:1632–1633.
8. Bhatta KM, Rosen DI, Dretler SP. Acoustic and plasma-guided laser angioplasty. Lasers Surg Med 1989; 9:117–123.
9. Deckelbaum LI, Lam JK, Cabin HS, Clubb KS, Long MB. Discrimination of normal and atherosclerotic aorta by laser-induced fluorescence. Lasers Surg Med 1987; 7:330–335.
10. Leon MB, Lu DY, Prevosti LG. Human arterial surface fluorescence: Atherosclerotic plaque identification and effects of laser atheroma ablation. J Am Coll Cardiol 1988; 12:94–102.
11. van Leeuwen T, van der Veen MJ, Verdaasdonk RM, Borst C. Noncontact tissue ablation by holmium: YSGG laser pulses in blood. Lasers Surg Med 1991; 11:26–34.
12. Haase KK, Baumbach A, Wehrmann M, Duda S, Cerullo G, Rückle B, Steiger E, Karsch KK. Potential use of holmium lasers for angioplasty: Evaluation of a new solid-state laser for ablation of atherosclerotic plaque. Lasers Surg Med 1991, 11:232–237.
13. Walsh JT, Deutsch TF. Er:YAG laser ablation of tissue: Measurement of ablation rates. Lasers Surg Med 1989; 9:327–337.
14. Srinivasan R. Ablation of polymers and biological tissue by ultraviolet lasers. Science 1989; 234:559–565.
15. Haase KK, Hanke H, Baumbach A, Wehrmann M, Rose CH, Karsch KK. Quantification of pressure waves during ablation of normal arterial wall and atherosclerotic plaque by excimer lasers. Z Kardiol 1993; 82:87–93.
16. Li ZZ, Reinisch L, van der Merwe W. Bone ablation with Er:YAG and CO_2 laser: Study of thermal and acoustic effects. Lasers Surg Med 1992; 12:79–85.
17. van Leeuwen TG, van Erven L, Meertens JH, Motamedi M, Post MJ, Borst C. Origin of arterial wall dissections induced by pulsed excimer and mid-infrared laser ablation in pig. J Am Coll Cardiol 1992; 19:1610–1618.